Selective self-assembly at room temperature of individual freestanding Ag_2Ga alloy nanoneedles

Mehdi M. Yazdanpanah, Steven A. Harfenist, Abdelilah Safir, and Robert W. Cohn[a)]
The ElectroOptics Research Institute and Nanotechnology Center, University of Louisville, Louisville, Kentucky 40292

(Received 22 April 2005; accepted 12 August 2005; published online 5 October 2005)

Liquid gallium drops placed on thick Ag films at room temperature spontaneously form faceted nanoneedles of Ag_2Ga alloy oriented nearly normal to the surface. This observation suggests that single nanoneedles can be selectively grown by drawing silver-coated microcantilevers from gallium. Needles from 25 nm to microns in diameter and up to 33 μm long were grown by this method. These metal-tipped cantilevers have been used to perform atomic force microscopy (AFM) and AFM voltage lithography. © *2005 American Institute of Physics*. [DOI: 10.1063/1.2060930]

INTRODUCTION

The liquid metal gallium (Ga) rapidly dissolves many metals at and even below[1] its bulk melting temperature (29.8 °C). Liquid Ga can be supercooled to at least 58 °C below its melting point for extended periods of time.[2] At elevated temperatures and pressures gallium melts have been supersaturated with chemical vapors from which nanowires can nucleate and grow as vertical carpets,[3,4] which in some cases are composed of the vaporized elements alone,[3,5] and in other cases form oxide[5,6] and semiconducting[7] compounds with Ga. A number of metals have been reported to interdiffuse and react with Ga at room temperature, resulting in intermetallic compounds and ordered crystalline phases.[8,9] We have observed at and even below room temperature that Ga placed in contact with gold (Au) thin films reactively alloys forming crystallites of $AuGa_2$ surrounded by Ga-rich alloy.[10] The Ga-rich liquid continues to react and a wave front of the alloyed material is observed to spread over and continuously alloy with the Au film beyond the original Ga source. Above room temperature with the spreading rate accelerated, fractal-shaped, interconnected networks of Au-rich nanowires can form on the surface of the substrate.[11] From our ongoing experiments of Ga alloying with other metal thin films we have observed self-assembly processes that result in a number of other unusual morphologies.

Herein we report on the most intriguing of these results, which is the alloying of Ga with films of silver (Ag) at room temperature which results in rapid nucleation and growth of long crystalline alloy needles of nanometer diameter. Of greatest significance is that an individual needle can be directed to grow in a desired direction. An example of this concept and its experimental demonstration is presented in Fig. 1 where a silver-coated atomic force microscopy (AFM) tip[12] is dipped[13] into a *liquid* drop of Ga *at room temperature*.[2] The Ga readily adheres to the Ag coating, forming a meniscus on partial retraction of the tip. With further retraction, the tip, with a freshly grown needle attached, breaks free from the Ga. In some experiments a longer initial retraction distance creates a longer meniscus that thins over time, draining away the Ga to expose a single needle. Immersion of the tip in the Ga for 2 min usually results in the formation of a needle, and even a few seconds of immersion frequently results in the formation of a needle.

Qualitative observations of and assumptions about the process of forming needles are summarized in the schematic illustration in Fig. 1. We assume that the localization of the needle to the tip is associated with both the presumed longitudinal concentration gradient of Ag that is dissolved from the tip [Fig. 1(b)] and the transverse localization of the narrow meniscus [Fig. 1(c)]. Figures 1(c) and 1(d) indicate the possibility of a number of needles forming with a single needle extending past the others. A small number [as in Fig. 2(a)] to a large number of needles have been observed to form in different experiments (with more needles being produced when the Ag films are thicker.) The cartoon portion of Fig. 1(d) shows another feature, which is the large amount of Ga that can adhere to the tip. Over time the Ga continues to reactively spread and alloy with the Ag of the cantilever forming a grainy pattern of Ag_2Ga crystallites over the cantilever surface. The continued spreading of the Ga eventually removes the excess unreacted Ga, which eventually uncovers and makes visible all the nanowires formed at the tip. We have also formed freestanding needles at the end of tipless cantilevers and produced single needles of both parallel and normal orientations to the cantilever surface.

Before describing additional details of the process for forming alloy needles on AFM cantilevers and demonstrating their applicability to scanning probe microscopy, it is helpful to consider our original observations of spontaneous needle formation when Ga is placed on top of thin and thick films of Ag. It was these observations that originally suggested the single-needle fabrication process.

NEEDLE FORMATION FROM SILVER FILMS

We first observed spontaneous growth of alloy needles when we placed lines of liquid gallium on sputtered Ag thin films (thicknesses from 15 to 305 nm) on silicon substrates. A sharpened tungsten probe (7 μm tip radius) mounted in a

[a)]Electronic mail: rwcohn@uofl.edu

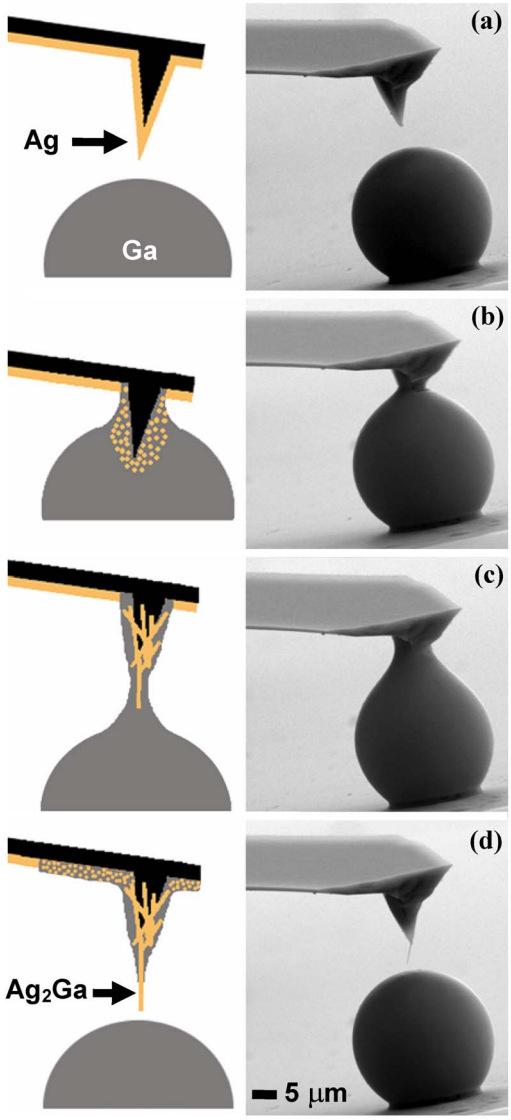

FIG. 1. (Color online) Process for freestanding needle fabrication: (left column) schematic and (right column) demonstration as recorded in time-sequential SEM images. (a) An AFM probe that is Ag coated (50–200 nm) is positioned over a melted or supercooled liquid drop of Ga between 15 and 25 °C. The nominally 10-nm-thick Cr underlayer is included to promote adhesion of the resulting needle. (b) A portion of the cantilever is dipped into the drop dissolving Ag into the Ga. (c) The cantilever is retracted and held from 2 s to 2 min (in the experiment shown 5 s was used) while the needles form. (d) Then the cantilever is either retracted further or the Ga recedes to free the needle-tipped cantilever from the Ga drop.

micromanipulator[13] is dipped into liquid Ga until a drop of the metal adheres to it. The hanging drop is touched to the Ag film surface and scanned laterally, forming a line of liquid Ga of width from 30 to 100 μm and from 0.5 to 10 μm thick. Within seconds surface-oriented alloy needles appear within the liquid Ga, first nucleating near the edges and growing in toward the center of the line. Thereafter, needles form near the center and parallel to the line of Ga. The needles continue to nucleate and grow until the Ga is depleted by the formation of needles inside the line and through lateral diffusion and alloying of Ga outside the line. The Ag film outside the Ga line transforms to a grainy texture due to the formation of alloy nanocrystals. The reaction can proceed from 1 to 3 days until Ga is no longer visible around the needles.

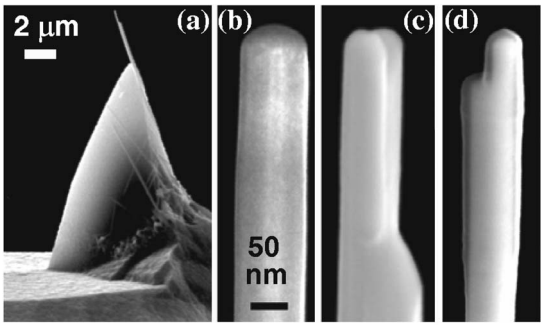

FIG. 2. Needles formed on cantilevers by the process of Fig. 1 (SEM images). (a) Closeup of the cantilever tip and attached needle from Fig. 1 and [(b)–(d)] closeups of single needles formed on three different tips. The scale bar in (b) also applies to (c) and (d).

Figure 3(a) shows scanning electron microscopy (SEM) images of the needles for Ag film thicknesses of 30, 127, and 305 nm, respectively. Needles as small as 35, 90, and 95 nm are found in the respective trials. For a 15-nm-thick film, needles as small as 25 nm diameter were found. Figure 3(a) (30 nm) shows that the needles are still surrounded by a layer of Ga. The openings through the Ga show the chromium (Cr) underlayer on the substrate. The Ga can be completely depleted over time by continued reactive spreading through the surrounding Ag film. Any remaining Ga can be removed with 1.0*M* HCl at 60 °C or 0.57*M* HF at room temperature. In Fig. 3(a) (127 nm) the Ga has been completely reacted with the thicker Ag film resulting in a number of layers of needles and thicker needles. In Fig. 3(a) (305 nm) the needles are even thicker and faceting is evident on the thickest needles. A noticeable minority of the needles that cross grow together, making it difficult to release a large fraction of the needles by HCl etching. When ultrasonication is used, segments of the full needles can be broken from the mass of needles.

When liquid Ga that is 50–100 μm thick is similarly placed on a much thicker film (99.9% Ag foil, 127 μm thick from Alfa Aesar) needles again form. The Ga reaction can take from 2 to 7 days until all the Ga is consumed and produces the textured line in Fig. 3(b). The central portion of the line forms directly under where the Ga had been originally placed. The closeup of this central region [Fig. 3(c)] shows that the nanowires are decidedly vertical in orientation. It appears to us that the needles grow parallel to the direction of movement or flow of the Ga and that at the center of the line, the Ga is moving downwards through the foil.

Additional evidence of vertical growth of needles on thick foils is observed prior to the complete depletion of the Ga. Specifically, Figs. 3(d) and 3(e) show individual needles that have grown through an ~3-mm-thick layer of Ga after 1 day. If the same experiment is performed at 240 °C instead of room temperature, faceted vertical needles again form though this time of larger diameter [Fig. 3(f)]. The increased diameter appears to be related to the effect of increased diffusion rate as described by nucleation theory.[14] It is these

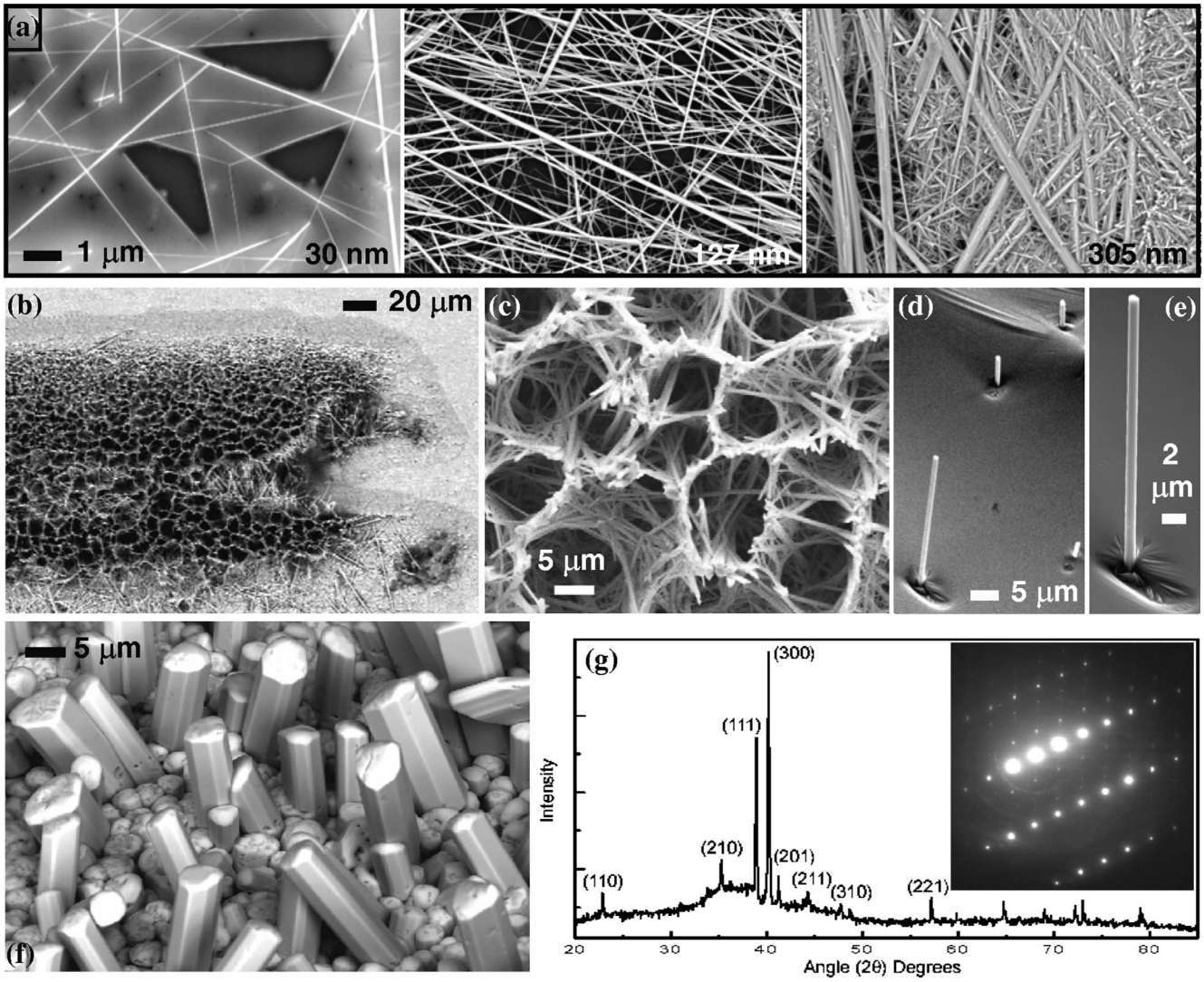

FIG. 3. Spontaneous needles that form when Ga is applied to sputtered Ag films. (a) Needles formed on 30-, 127-, and 305-nm-thick Ag films after a thin line of Ga is drawn over Ag on the end of a tungsten needle. When the film is much thicker (127 μm Ag foil) the Ga reacts to produce (b) needles of a nearly vertical orientation at the center of the line of Ga. (c) Closeup of the nearly vertical needles in the center of line in (b). (d) Needles that protrude through the Ga early in the reaction, before the Ga completely reacts with the Ag foil. (e) Closeup of one of the needles in (d). (f) The thicker needles that form when the reaction is performed at 240 °C instead of room temperature. (a)–(f) are SEM images. (g) X-ray-diffraction pattern from needles grown on a thin film of Ag. (Inset) SAD (selected area diffraction) pattern from a single needle that shows that single needles are highly crystalline.

various observations related to Fig. 3 that suggested the possibility of obtaining oriented single-needle growth by confining the growth to a thin meniscus of Ga [as illustrated in Fig. 1(c)].

X-ray-diffraction (XRD) analysis with the Cu $K\alpha$ line ($\lambda = 1.54$ Å) is performed on needles grown under conditions similar to those in the samples shown in Fig. 3(a).[15] The XRD [Fig. 3(g)] identifies the crystals as the ordered ζ' phase of the Ag–Ga phase diagram.[9,16] From the XRD we calculated the lattice parameters of 7.75 and 2.87 Å for a and c, respectively, for this hexagonally close-packed crystal. The parameters are within 0.2% of the values reported by Gunnaes *et al.* for their 10-μm-diameter faceted needles of the ζ' phase with stoichiometry of Ag_2Ga that they grew by slow cooling from a Ga-rich melt.[9] Their crystals are similar in appearance to the needles in Fig. 3(f). Additionally, Simic and Marinkovic noted from the XRD the stable formation of the ζ' phase at room temperature when sandwiches of the thin films of Ga and Ag were brought into contact with each other.[17] Several single freestanding needles formed on AFM cantilevers were examined by energy dispersive x-ray spectroscopy (EDS) in a SEM and found to be 2:1 Ag:Ga stoichiometry, even though the Ag–Ga phase diagram shows that the stoichiometry of the ζ' phase is not single valued. Also, the needles formed by the Ag–Ga reaction are highly crystalline, as demonstrated by the selective area electron-diffraction (SAD) pattern shown in the inset of Fig. 3(g) from a single needle of 200 nm diameter.[18] The SAD of the needle in Fig. 4 also produces a diffraction pattern with narrow diffraction peaks, indicating that this freestanding needle is crystalline, as well. While it was not possible to tilt the 10°-tilted AFM tip and needle into the same orientation as the needles on transmission electron microscopy (TEM) grids, we are convinced that the freestanding Ag_2Ga needles

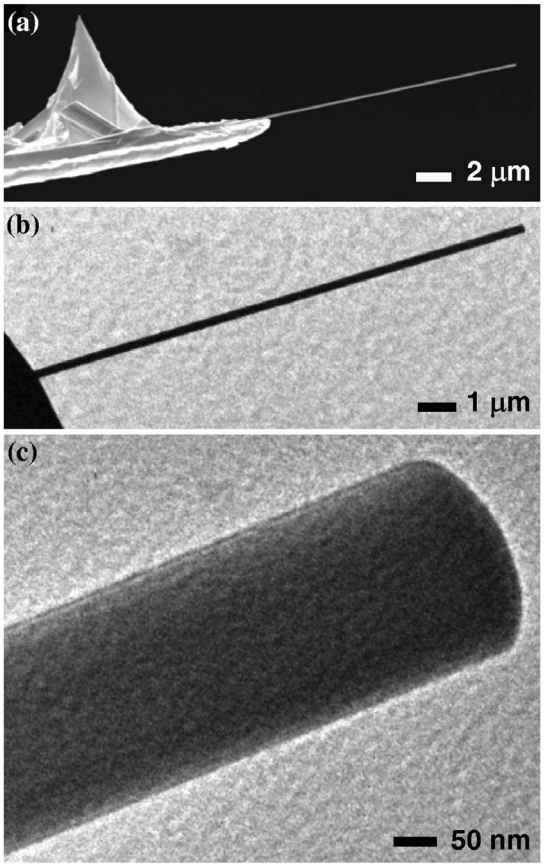

FIG. 4. Single needle that was selectively grown parallel to the surface of the cantilever. (a) SEM image of the ~250-nm-diameter needle showing that it protrudes 14 μm beyond the end of the cantilever. Closeup TEM images of (b) the entire length of the needle beyond the cantilever and (c) the end of the needle. These images show that the needle is of nearly constant diameter.

are identical in composition to surface-grown needles (based on the EDS analyses of each) and that both are crystalline (based on SAD analyses).

SELECTIVE GROWTH AND ORIENTATION OF SINGLE NANONEEDLES

At this point we resume and complete the description of the selective formation of individual freestanding alloy needles. Orientation of the needles is controllable as illustrated by forming needles that are oriented normal to the AFM tip (Figs. 1 and 2), parallel to the cantilever surface (Fig. 4), and normal to the surface of a tipless cantilever (Fig. 5). The needles in Figs. 1 and 2 were drawn from a spherical drop of Ga that is resting on a silicon substrate. This shape occurs after the Ga drop is immersed in 1.0*M* HCl at room temperature for 1 min or 0.57*M* HF at room temperature for 2 min. Then the sample is blown dry with nitrogen and immediately inserted into the SEM chamber. Without the acid treatment, the Ga has a low contact angle on the order of 25° or less and a somewhat irregular boundary [e.g., in Figs. 5(a)–5(c)]. The change in contact angle with etching is attributed to the removal of a nanometer thick Ga_2O_3 layer[19] that grows on the Ga surface under ambient conditions. The oxide is thin enough that it does not seem to affect the ability to penetrate the surface or the formation of the needles on retraction. A patch of the oxide film can sometimes be detached from the pool and transferred to the end of the needle.

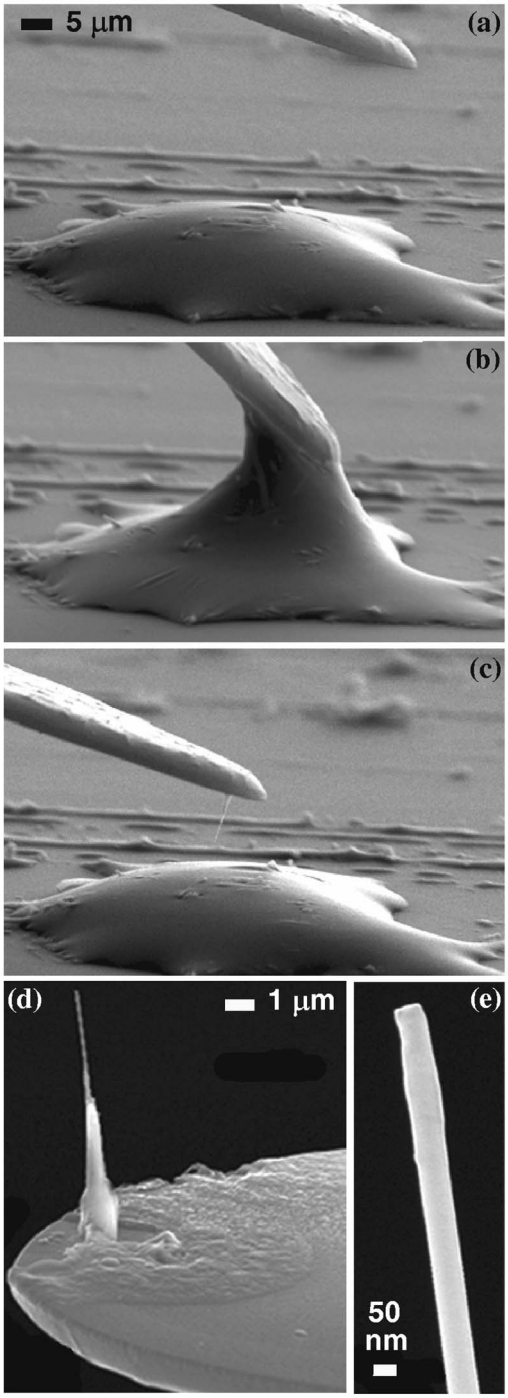

FIG. 5. Demonstration of the single-needle fabrication process on a tipless cantilever. [(a)–(c)] A sequence of SEM images that show the fabrication of the needle. (d) A closeup of the cantilever in (c) that shows that most of the Ag film has been removed around the base of the needle. (e) A further closeup of the needle formed on the cantilever. The end of the needle is 55 nm in diameter.

The needle in Fig. 4(a) was grown parallel to the surface of a Ag-coated (10 nm Cr and 90 nm Ag) cantilever by immersing the tip and the flat surface of the cantilever in a drop of Ga (as in Fig. 1). Then immediately afterwards, the

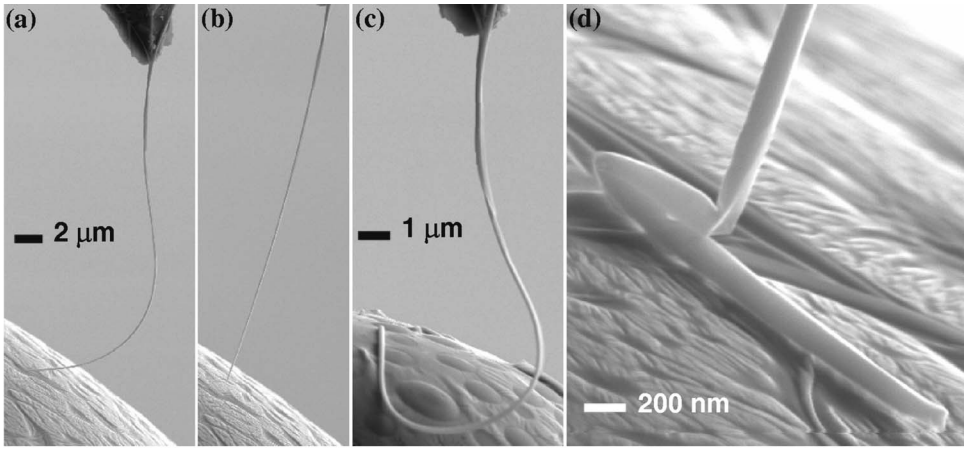

FIG. 6. Mechanical properties of the highest aspect ratio needle from this study (SEM images.) (a) Needle that has been forced to buckle by pressing it against the Ga droplet from which it was originally drawn. (b) Recovery of needle to its nearly linear form after removal of the force. (c) The same needle flexed to an even greater degree than in (a). The needle, shown on a different droplet than in (a) and (b), also recovers its linear form upon the removal of the applied force. While (a)–(c) show the needle to be 29 μm long, the original needle was 33 μm long. In our first test of buckling with this needle there were (d) elastic failures which kinked and broke off 4 μm of the needle. The needle is shown on the same droplet as in (a) and (b). The textures on the surface of the spherical Ga droplets are due to reformation of the surface oxide after chemical removal of the native oxide.

cantilever was pulled laterally along the drop, forming a meniscus between the drop and the end of the cantilever. After holding the needle in this position for 2 min the needle was released from the Ga pool through further lateral pulling. This produces a freestanding needle of 250 nm diameter that extends 14.1 μm past the end of the cantilever. It is remarkable that the needle is of nearly constant diameter over its entire length, as shown in the TEM images in Figs. 4(b) and 4(c).

We also produced a needle of even higher aspect ratio (Fig. 6) which was 130 nm diameter over approximately half of its 33 μm length using the geometry of Fig. 1. The needle resulted after inserting the end of the tip inside the Ga and pulling up a meniscus. This was held for 2 min during which time the meniscus receded back into the drop leaving an exposed needle of about 200 nm diameter. The cantilever was further retracted to expose 10 μm of the needle, leaving an additional length submerged in the Ga. After another 8 min the needle was completely removed from the drop exposing the thinner portions of the needle. Note that the needle length greatly exceeds the length of the meniscus. That is, the meniscus sets the conditions to initiate single-needle growth, but then the needle can continue to grow well beyond the meniscus region. Also, adhesion of the needle to the Ga is weak enough that long needles can usually be removed without breaking them.

Figure 6 shows the flexibility of 29 μm of the same needle as it is pushed against Ga droplets [Fig. 6(a)] and then released [Fig. 6(b)] to a nearly unbent position. This flexing was repeated several times without destruction and even more severe beam bending and buckling was achieved in Fig. 6(c). However, the first attempt to bend the needle [in the identical configuration as in Figs. 6(a) and 6(b)] did produce plastic deformation, kinking, and breaking off of 4 μm of the needle. The broken section is shown in Fig. 6(d).

A needle also was formed nearly normal to the surface of a tipless cantilever coated with 90 nm of Ag (Fig. 5). Figures 5(a)–5(c) show the time lapse images. The end of the cantilever was immersed in the Ga and then retracted to form the meniscus in Fig. 5(b). Note the strong adhesion of the Ga to the underside of the cantilever. After holding the cantilever at this position for 2 min, the cantilever is retracted further until the needle snaps free from the Ga, resulting in the needle in Fig. 5(c). The closeups of the needle in Fig. 5(d) show that the Ag has been dissolved from the end of the cantilever, and additional interaction of the Ga with the Ag is noted in that the film is roughened in the vicinity of the needle. The further closeup in Fig. 5(e) shows that the diameter of the needle is 55 nm.

POTENTIAL APPLICATIONS OF THE SELECTIVELY GROWN NEEDLES

We have begun evaluating needle-tipped AFM cantilevers for AFM profiling and AFM voltage lithography. The needles were grown by the method of Fig. 1 on tipped and tipless AFM cantilevers and used both in contact and tapping modes. Initially, when the needles were grown directly on a silicon (Si) cantilever, the needle could easily be detached during scanning. With the addition of the 10 nm Cr underlayer, the needles usually adhere to the tip indefinitely. For example, continuous scanning in both contact mode[20] (3-μm-long needle of 400 nm diameter) and tapping mode[21] (120-nm-diameter needle tip of 4 μm length) was performed for 14 h without dislodging the tip and with no change in resolution. Needles with lengths of less than 5 μm are used due to their improved stability and resistance to buckling. To further reduce the possibility of a needle buckling in tapping mode, the z-piezo set point is adjusted to go into feedback with 10% damping of the cantilever oscillation amplitude, instead of the manufacturer recommended set point at 20% damping.

Figure 7(a) is a tapping-mode topography scan[22] of a sputtered Au thin film (nominally 50 nm thick) that shows the individual film grains. Figure 7(b) shows the image of a similar area on the same film as recorded in a field-emission-

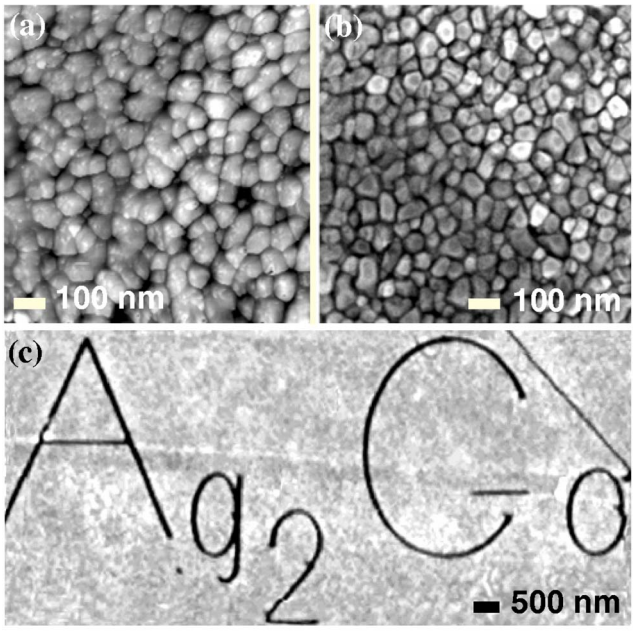

FIG. 7. Evaluations of the needle-tipped cantilevers for AFM applications. (a) AFM topography image of a thin sputtered Au film using a 120-nm-diameter needle-tipped cantilever. (b) SEM image of a similar looking area of the same film. Comparison of the two images, as described in the text, leads to an estimate that the tip resolution is 14 nm on this sample. (c) AFM image of pattern written with a needle-tipped cantilever by voltage lithography of a thin PMMA film.

SEM (FE-SEM, 1 nm beam diameter). Autocorrelations of the topography image corresponding to Fig. 7(a) and the grayscale image in Fig. 7(b) are calculated to estimate the average grain sizes and from this data determine the loss in resolution due to the finite diameter of the needle. The grain size and resolution loss are reported at 0.707 times the full width at half maximum of the autocorrelation peak. The average diameters for the AFM scan and the SEM image are 28 and 21 nm, respectively. The autocorrelation function of the SEM is best fitted to the AFM autocorrelation function when a Gaussian function with spread corresponding to a 14 nm [i.e., this width is 0.7 full width at half maximum (FWHM) of the Gaussian] is used. Thus, we consider the resolution loss to be around 14 nm for this particular sample. On another portion of the same sample we profiled with the same needle and also with a Si cantilever (same probe as Ref. 22). In this region the grains were larger and steeper, and the resulting diameters found by the autocorrelation procedure were 47 and 32 nm, respectively. The resolution loss as compared to the Si cantilever is 34 nm for this sample.

Conductive AFM probes are useful for voltage nanolithography.[23] The nanoneedle and the silver coating on the cantilever form a highly conductive path that is suitable for applying constant current through an insulating resist. In our experiments (in a Veeco M5 AFM) we spun on a 123-nm-thick film of electron-beam resist PMMA (4 wt % polymethyl methacrylate in Anisole solvent, MicroChem Corp., Newton, MA) onto a Si substrate that is sputter coated with a 20-nm-thick Au coating and a 5 nm Cr adhesion layer. The sample was prebaked at 150 °C for 5 min in a convection oven. The 120-nm-diameter needle on a tipless cantilever (same as Ref. 20) was used in tapping mode (average height above surface of ~12 nm) and scanned at a tip velocity of 300 nm/s. The tip was biased to apply 150 pA constant current. The exposed pattern was then developed in a 2:1 methyl isobutyl ketone (MIBK) to isopropanol solution for 90 s. An AFM topography image[24] of the lithography pattern is shown in Fig. 6(c). The depth of the exposed trenches measures 35 nm and the linewidths are as small as 100 nm. In a second exposure experiment on a 40-nm-thick PMMA film was exposed with a 60-nm-diameter needle grown on a tipless cantilever[25] and scanned in tapping mode at a tip velocity of 200 nm/s with a 200 pA exposure current. The depth of the exposed trenches measures 9 nm and the linewidth is as small as 30 nm and no larger than 80 nm [as measured by AFM (Ref. 24)]. Further adjustment of dose and development time will be required to completely develop through the resist. One of the most encouraging aspects of the needles for use in voltage lithography is the greater stability of the applied voltage as compared to thin metal-film-coated AFM tips, which shows up as more uniform control of linewidths in our exposures. The problem with the thin-film metallized Si tips is that the metal rapidly wears off the end of the tip resulting in a poorly defined electrical path from the edge of the remaining film. With a metallized (5 nm Cr adhesion layer and 20 nm Au) Si cantilever the initial voltage (at constant current) was 1 V and the voltage rose to 8 V within 10 min. For the needle-tipped cantilever, the initial writing voltage (at constant current) was 1 V and the voltage stayed constant for 10 min and increased to 4 V over 1 h. With the needle-tipped cantilevers we have continuously written for over 1 h with no change in resolution.

DISCUSSION: DESCRIPTIVE MODEL OF THE GROWTH PROCESS

In this section we compare our qualitative observations of Ag_2Ga needle growth with standard descriptive models[26–28] of alloy solidification. This discussion is intended to (1) relate several experimental observations from this study with the standard models and (2) suggest further studies that should result in a quantitative model of the growth process of the single freestanding needles.

Alloy solidification frequently begins with nucleation.[26] For alloy melts there is usually an activation energy barrier to homogenous nucleation. Heterogeneous nucleation (e.g., on seed particles, surfaces, and crevices) can reduce or even eliminate the activation energy barrier. Nuclei that exceed a critical radius then grow spontaneously, with a maximum growth rate when feature sizes are around twice the critical radius. A steady-state model of the longitudinal growth of needle-shaped precipitates from a supersaturated solution is presented in Ref. 27. It is based on the Gibbs-Thomson effect or the increase in free energy at the end of the small needle as compared to the bulk material. The excess free energy sets up a diffusive flow of solute towards the end of the needle that sustains the lengthening of the needle. Also, planar solid-liquid interfaces can become unstable (under the condition referred to as constitutional supercooling) and evolve

into cellular structures (e.g., lamellae, dendrites, or needles,) with growth similarly sustained by diffusion to the ends of the structures.[28]

In our experiments with tipped AFM cantilevers, needle growth appears to start after the AFM tip is retracted [Fig. 1(c)]. This produces a low contact angle between the Ga and Ag coatings. From the tip point, up to the atmosphere/Ga/Ag triple point, we find that the Ag film is completely dissolved away to the chrome underlayer. Upon removal from the Ga, we observe that the needles originate from the Cr–Ag ledge. Therefore the Cr–Ga ledge could be considered to be a crevice which lowers the energy barrier to nucleation. However, it is also possible that nucleation begins prior to the formation of the ledge, and that the low wetting angle of the Ga on the Ag resembles a crevice.

From a few to many needles can grow from this region of the AFM tip. As they lengthen they can grow into each other to form a bundle. As the bundle lengthens further it usually tapers down to a single needle that continues to grow well beyond the bundle. This tapering may be related to decrease of available solute, together with the instability of this material system to maintain planar fronts [e.g., illustrated by Figs. 3(b) and 3(c)]. That is, more Ag will diffuse to an isolated protrusion, enhancing the growth rate of a single needle over the larger diameter (i.e., more planar) bundle. In that the growth follows the longitudinal axis of the meniscus (e.g., in Figs. 1, 4, and 5) and reflects the diffusive flux set up by the needle tip, but this preferred growth direction may be further enhanced by longitudinal capillary and diffusive flow through the narrow meniscus.

The above description of needle growth has many of the features from standard models of alloy solidification and growth, with the addition of (eventual) single-needle growth in a selected orientation. Therefore, we expect that needle growth rate and morphology follow the mathematical models used for alloy growth.[26–28] These models depend strongly on temperature and temperature gradients, and thus experiments as a function of these variables can be conceived to quantify and optimize the needle growth process.

CONCLUSIONS

In summary, single freestanding nanoneedles of Ag_2Ga (at least as small as 25 nm diameter) can be spontaneously formed at room temperature by dipping a silver-coated surface into liquid Ga. Needles of horizontal and normal, as well as arbitrary, orientations have been formed on AFM cantilevers. Initial experiments show that the needle-tipped cantilevers can be used to perform AFM topography measurements and voltage lithography. While the resolution of these needle-tipped probes has not been as high as with silicon, the wear of the needles seems to be much less than the wear of the sharpened silicon tips. Continued studies at producing narrower needles should further improve the resolution of these probes.

ACKNOWLEDGMENTS

Partial research and equipment support for this study was provided by NASA (NCC5-571), NSF (ECS-0216347), and ARO (DAAD19-01-1-0489).

[1] I. A. Sheka, I. S. Chaus, and T. T. Mityureva, *The Chemistry of Gallium* (Elsevier, New York, 1966), p. 3.
[2] L. J. Briggs, J. Chem. Phys. **26**, 784 (1957).
[3] M. K. Sunkara, S. Sharma, R. Miranda, G. Lian, and E. C. Dickey, Appl. Phys. Lett. **79**, 1546 (2001).
[4] Z. W. Pan, S. Dai, D. B. Beach, and D. H. Lowndes, Appl. Phys. Lett. **83**, 3159 (2003).
[5] G. Bhimarasett, M. K. Sunkara, U. M. Graham, B. H. Davis, C. S. Suh, and K. Rajan, Adv. Mater. (Weinheim, Ger.) **15**, 1629 (2003).
[6] S. Sharma and M. K. Sunkara, J. Am. Chem. Soc. **124**, 12288 (2002).
[7] C.-C. Chen and C.-C. Yeh, Adv. Mater. (Weinheim, Ger.) **12**, 738 (2000).
[8] V. Simic and Z. Marinkovic, Thin Solid Films **209**, 181 (1992).
[9] A. E. Gunnaes, O. B. Karlsen, and P. T. Zagierski, J. Alloys Compd. **297**, 144 (2000).
[10] M. M. Yazdanpanah, S. Chakraborty, S. A. Harfenist, R. W. Cohn, and B. W. Alphenaar, Appl. Phys. Lett. **85**, 3564 (2004).
[11] M. M. Yazdanpanah, S. A. Harfenist, and R. W. Cohn, Appl. Phys. Lett. **85**, 1592 (2004).
[12] BudgetSensors BS-Multi75 AFM probe (60 kHz and 3 N/m) sputter coated on the tip side with a 10 nm Cr adhesion layer and a 100 nm Ag film.
[13] The tip is manipulated using a manually controlled three-axis Fullam micromanipulator that is mounted through the chamber wall of the SEM. The use of the micromanipulator and the vacuum environment of the SEM is not a necessity, but is only used to observe the process and record the images for this paper.
[14] J. P. Schaffer, A. Saxena, S. D. Antolovich, T. H. Sanders, Jr., and S. B. Warner, *The Science and Design of Engineering Materials*, 2nd ed. (McGraw-Hill, New York, 1999), p. 298.
[15] Silver is sputtered to a thickness of 300 nm on a glass slide. Gallium is spread over the entire sample and then immediately placed in the x-ray diffractometer with the measurement being completed within an hour.
[16] B. Predel, in *Phase Equilibria of Binary Alloys*, edited by O. Madelung (CD-ROM, Springer, 2003).
[17] V. Simic and Z. Marinkovic, Thin Solid Films **209**, 181 (1991).
[18] SAD was performed in a transmission electron microscope (TEM) at normal incidence to the grid and needle. The needle was grown on an ultrathin carbon, 400 Cu mesh TEM grid (Pelco). A sub-10-nm Cr adhesion layer and a 50 nm layer of Ag were sputtered on the grid. A small drop of Ga placed on the film reacted for several days to produce a sparse pattern of needles that could be probed individually by the TEM beam.
[19] M. J. Regan, H. Tostmann, P. S. Pershan, O. M. Magnussen, E. DiMasi, B. M. Ocko, and M. Deutsch, Phys. Rev. B **55**, 10786 (1997).
[20] Veeco tipless ultralever contact probe B, 1.1 N/m spring constant, and 78.1 kHz resonance frequency, imaged in an Asylum Research MFP-3D AFM at 15 μm/s scan speed over a 25 μm^2 area with a set point of 1.3 nN.
[21] Veeco tipless ultralever noncontact D, 50 N/m spring constant, and 354.7 kHz resonance frequency, in a Veeco CP AFM with a 5 μm scanner at 4.8 μm/s over a 2 μm^2 area.
[22] BudgetSensors BS-Multi75 AFM probe (60 kHz and 3 N/m), needle-tip radius of curvature 40 nm, and overall needle length of 3.3 μm. The tip radius of the Si tip is less than 10 nm.
[23] K. Wilder, H. T. Soh, A. Atalar, and C. F. Quate, Rev. Sci. Instrum. **70**, 2822 (1999).
[24] BudgetSensors BA-Tap300 tapping-mode probe at 319 kHz and 40 N/m. The tip radius is less than 10 nm.
[25] Veeco tipless cantilever model ULCT-NTNM, D type with resonance frequency of 155 kHz and spring constant of 5 N/m.
[26] D. A. Porter and K. E. Easterling, *Phase Transformations in Metals and Alloys* (Nelson Thornes, Cheltenham, UK, 1992), pp. 186–197.
[27] D. A. Porter and K. E. Easterling, *Phase Transformations in Metals and Alloys* (Ref. 26), pp. 283–285.
[28] D. A. Porter and K. E. Easterling, *Phase Transformations in Metals and Alloys* (Ref. 26), pp. 214–222.